

# Moment curvature method for fire safety design of steel beams

H.X. Yu† and J.Y. Richard Liew‡

*Department of Civil Engineering, National University of Singapore,  
Blk E1A, 1 Engineering Drive 2, Singapore 117576*

*(Received January 3, 2004, Accepted April 30, 2004)*

**Abstract.** This paper presents a moment-curvature method that accounts for the strength deterioration of steel at elevated temperature in estimating the response of steel beams exposed to fire. A modification to the EC4 method is proposed for a better estimation of the temperature distribution in the steel beam supporting a concrete slab. The accuracy of the proposed method is verified by comparing the results with established test results and the nonlinear finite element analysis results. The beam failure criterion based on a maximum strain of 0.02 is proposed to assess the limiting temperature as compared to the traditional criteria that rely on deflection limit or deflection rate. Extensive studies carried out on steel beams with various span lengths, load ratios, beam sizes and loading types show that the proposed failure criterion gives consistent results when compared to nonlinear finite element results.

**Key words:** elevated temperature; fire safety design; limiting temperature; moment-curvature method; steel beam; limit state design.

---

## 1. Introduction

Modern fire resistance design codes (BSI 2000 and CEN 2001) provide mainly two simplified methods for the design of beams in fire, namely the standard fire test method and the moment capacity method. In the standard fire test method, a simply-supported load-bearing member is heated in a furnace with gas temperatures following a standard time-temperature curve. The time taken for the member to reach a prescribed failure criterion is the fire resistance rating of the member. This method is rather time consuming and costly because any change to the types of structural members, supporting conditions and applied loads would require additional tests. Simplified design charts and tables have been produced for the prediction of the fire resistance of individual members based on a limited number of full-scale tests (Buchanan 2001).

The moment capacity method calculates the load bearing capacity of a member at elevated temperatures according to the temperature distribution in the member and the corresponding strength reduction factors. This method is based on ultimate strength analysis and the deformation of member is not considered. However, there are situations where the deformation criteria shall be applied when the means of protection or the design criteria for separating members require consideration of the

---

†Ph.D. Scholar

‡Associate Professor

deformation of the load bearing structures (Lawson *et al.* 1996). Eurocode 3 Part 1.2 deals with this requirement by using a modified reduction factor, which corresponds to approximately 0.5% strain in the steel members so that the deflections are unlikely to exceed span/100. This method triggers one of the major criticisms about ENV version of EC3 because of its (1) open end formulation, (2) lack of functional background, and (3) exceptional material for steel (Twilt 2001). For a performance-based design to meet the real design requirements, the deflection history of the beam should be calculated.

Although recent research has been directed to the investigation of the effect of structural continuity on the design of floor beams (Wang 2001, Li *et al.* 2000, Liu *et al.* 2002, etc), it is simpler to idealize beams as individual members for the purpose of design. Even though beam's catenary action has been well investigated, it is still not possible for all beams to be left unprotected and remained stable by catenary action (Huang *et al.* 2004). This is particularly true for beams supporting compartment walls. They are designed to satisfy certain limiting deflection criteria when exposed to fire in order to prevent the spread of fire from one compartment to another. Although advanced nonlinear analysis methods have been developed for analyzing large scale framework (Liew *et al.* 1998, 2002, Li *et al.* 1999, Liew and Ma 2004), their uses require careful verification. Guidance on the use of advanced calculation methods must be given before they can be fully implemented in practice. On the other hand, the conventional approach based on simplified calculation method offers a flexible and reasonable approach for checking the limit states of individual members in the whole framework.

In this paper, the effect of temperature distribution in the cross section on the structural behaviour of steel beam is firstly discussed. Suggested improvements are made to the EC4 method in estimating the temperature distribution of I-section beams supporting concrete slabs and the results obtained are verified against test results. A moment-curvature method is then proposed to estimate the deflections of steel beams at elevated temperatures, which, when combined with the thermal bowing deflection due to the temperature gradient in the cross section, gives the total deflection history of the beams. The calculated deflection is compared to established test and numerical results and the accuracy of the proposed method is verified. The beam failure criterion based on the maximum strain of the beam section reaching the effective yield strain of 0.02 is proposed to calculate the failure temperature of beams. The results obtained are compared with those calculated from the conventional failure criteria based on the limiting deflection or the deflection rate. The proposed failure criterion is found to be consistent in predicting the failure temperature compared to nonlinear finite element results for a wide range of beam parameters such as different load ratios, section sizes and loading conditions.

## 2. Temperature distribution in beams

Temperature increase within structural members has two effects on the structural response behaviour. One is the reduction of materials strength and stiffness leading to a reduction in the load bearing capacity of the structural member. For example, steel losses about 89% of its yield strength and 91% of its elastic modulus at 800°C. Decrease in yield strength significantly reduces the ultimate load resistance of the member and a reduction of elastic modulus means larger strain is developed for the same stress state and thus large deformation is expected. The other effect is the strain due to thermal expansion and it will produce thermal deformation if the member is not restrained and will induce thermal stress if it is restrained. The real structural response could be complicated due to the multiple interactions between these two effects.

For steel beams engulfed in a compartment fire, it is rational to assume that temperature is uniformly

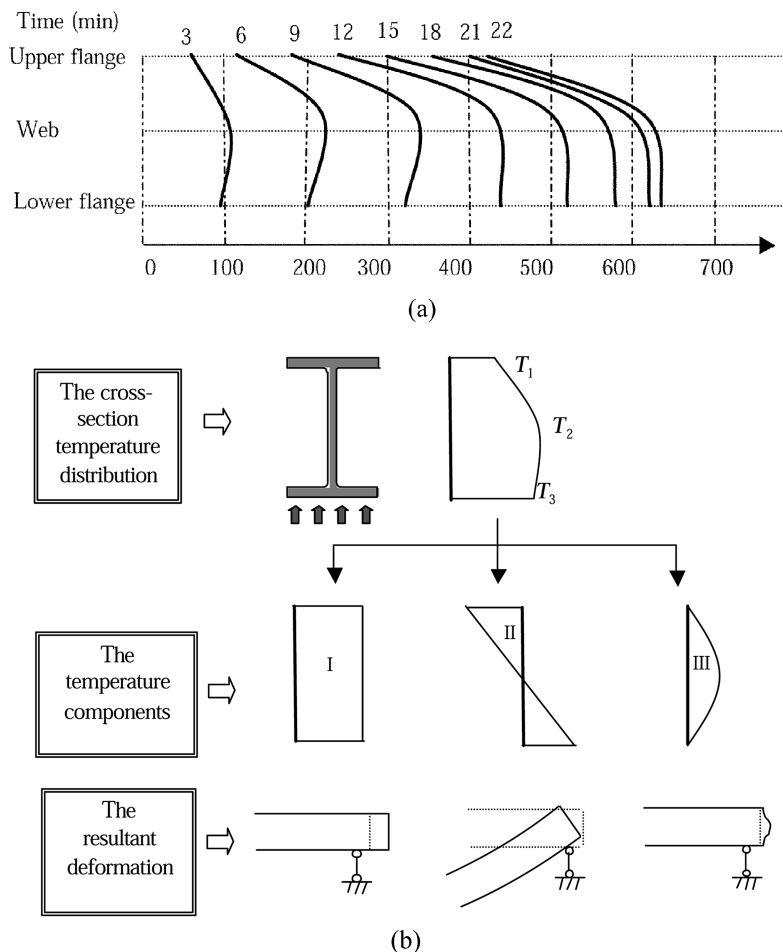


Fig. 1 (a) Temperature distribution over the cross-section from standard test results (Wainman and Kirby 1987, test 3), (b) Temperature components and their resultant deformation

distributed along the length of the member (Franssen *et al.* 1995). The temperature distribution over the beam section may be assumed to be uniform if it is heated from four sides due to the good conductivity of steel. Simplified method for estimating the steel temperature is given in Eurocode 3 (CEN 2001).

However, for steel beams that are supporting a concrete slab, the upper flange temperature will be somewhat lower. Fig. 1(a) shows a typical temperature distribution observed from the beam tests (Wainman and Kirby 1987). The response of beams exposed to fire may be attributed to three affecting factors. The first is due to uniform heating, which induces axial expansion. The second is due to linear temperature variation in the cross section, which induces curvature bending. These two factors do not produce internal stress if the beam is free to expand. The last influencing factor is due to non-uniform heating in the beam section. The resultant deformation and stress state are shown in Fig. 1(b). From the deflection point of view, the total temperature profile contributes to the loss of cross-section stiffness while only the temperature gradient produces additional thermal deflection.

Liew (2004) provides a means to estimate steel temperature development of protected and unprotected steel based on iteration over small time step. The method is based on the principle that heat

is transferred to the exposed surface of steel member and the temperature of the steel member will be uniformly increased due to the heat input. In a small time increment  $\Delta t$ , the temperature increase  $\Delta T$  can be calculated as

$$\Delta T = \frac{A_m \dot{h}_{con} + \dot{h}_{rad}}{V \rho c} \tag{1}$$

where  $A_m/V$  is the section factor for unprotected steel member and is the ratio of the exposed surface area to the volume of the member in unit length.  $\rho$  and  $c$  are mass and specific heat of steel, respectively.  $\dot{h}_{con}$  is the heat transfer due to the convection and is calculated as

$$\dot{h}_{con} = \alpha_c (T_f - T_s) \tag{2}$$

where  $\alpha_c$  is the convection coefficient,  $T_f$  and  $T_s$  are temperatures of the fire and the steel member.  $\dot{h}_{rad}$  is the heat transfer due to radiation and is calculated as

$$\dot{h}_{rad} = \epsilon_{res} \cdot 5.6710^{-8} \cdot ((T_f + 273)^4 - (T_s + 273)^4) \tag{3}$$

where  $\epsilon_{res}$  is the resultant emissivity.

This method could only handle sections with uniform temperature distribution. To calculate the temperature distribution in a steel section as shown in Fig. 2, the whole steel section is divided into three plate components and the temperature of each component is calculated according to the simplified method as recommended by Eurocode 4 (CEN 2002). And the section factor would be  $(2t_f + w - t_w) / (w \times t_f)$ ,  $2/t_w$  and  $(2t_f + 2w - t_w) / (w \times t_f)$  for the upper flange plate, web plate and lower flange plate, respectively.

The convection coefficient and radiation emissivity, although simply recommended by Eurocode 1 (EC1 1996) to be  $\alpha_c = 25 \text{ W/m}^2 \text{ K}$  and  $\epsilon_{res} = 0.5$  respectively, are actually quite complicated and dependent

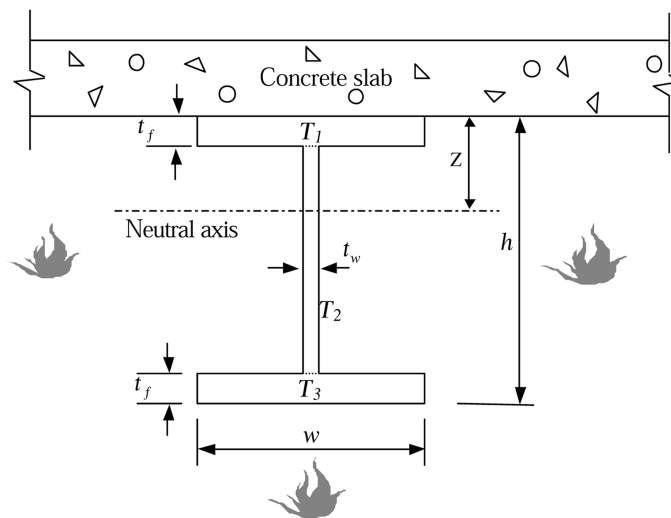


Fig. 2 The cross-section configuration for the upper flange, web and lower flange

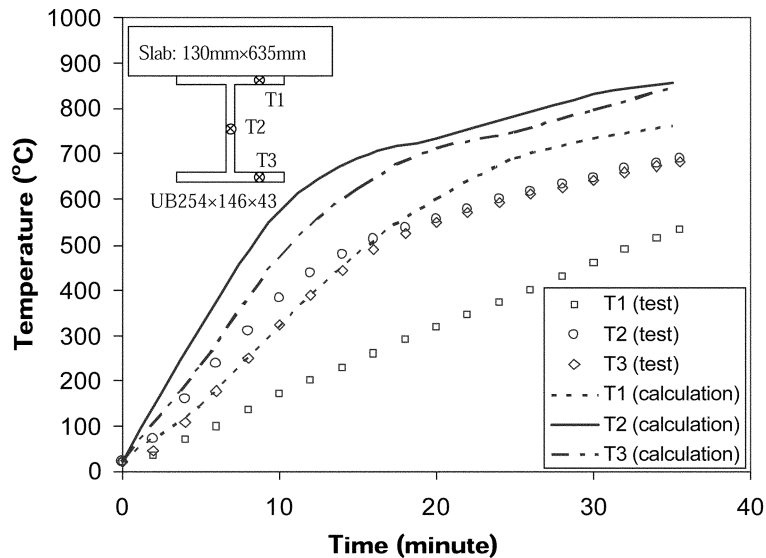


Fig. 3 The calculated method according to EC 4 against test results (Wainman and Kirby 1987, test 1)

on several factors (Wang 2002; Wong 2001). Fig. 3 shows the temperature profile of an I-section  $254 \times 146$ UB43 calculated using the Eurocode 4 (CEN 2002) procedure and the results are compared with the test results by Wainman and Kirby (1987). In general, the calculated temperatures are higher than the test results and the predicted temperature difference between the upper flange and lower flange is smaller than those observed from the test. The discrepancies are due to the fact that EC4 method does not consider the heat conductions between the cross-section plate components, including the heat sink effect of the concrete slab and over-simplification of the heat transfer coefficients. It has been proposed by Wong and Ghajel (2003) that the determination of the radiation emissivity has been treated as fudge factors to match experimental results rather than reflecting the true thermal properties related to the fire tests and any simple constant value will not be able to fit all test results. To provide a better estimation of temperature distribution in the steel section, the following modifications are proposed to the EC4 method:

1. The section factor of the upper flange is modified to  $(2t_f + kw - t_w)/(w \times t_f)$ . The heat flow into the upper flange through  $(1-k)w$  of the fire exposed edge is assumed to be lost to the concrete slab. The value of  $k$  is determined to be 0.3 by calibration against the test results from Wainman and Kirby (1987).
2. The resultant section factors from step 1 are further modified by 0.85, 0.6 and 1.25 for the lower flange, web and the upper flange, respectively, to account for the heat flux from the web and the lower flange to the upper flange.
3. The resultant emissivity  $\epsilon_{res}$  and convection coefficient  $\alpha_c$  are modified as a function of body temperature  $T$ :

$$\epsilon_{res} = 350/(T + 590) \quad (4)$$

$$\alpha_c = 8000/(T + 800) \quad (5)$$

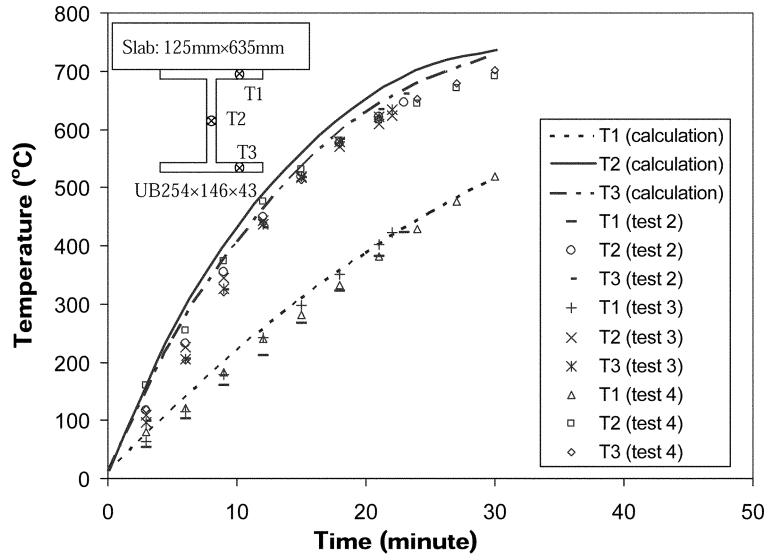


Fig. 4 The modified calculation method against test results (Wainman and Kirby 1987, tests 2, 3 and 4)

The calculated temperatures based on the above modification are in good agreement with test results for most of the 14 test results studied (Wainman and Kirby 1987). It is noted that tests on the same beam show some degree of variance in terms of temperature distribution; however, the calculated temperatures are slightly higher and hence conservative. For example, the calculated temperatures in Fig. 4 give conservative prediction for tests 2, 3 and 4 which are based on the same beam size 254×146UB43.

The proposed modifications made to the Eurocode 4 (CEN 2002) may be only appropriate for the fire exposed duration that is similar to the British standard tests. In predicting the response of steel beams, the modified method proposed in this section will be adopted. The deflection calculation method is applicable as long as temperature distribution is available regardless whether it is from test data or from any other calculation methods.

### 3. Deflection of steel beams at elevated temperature

For beams at normal temperature, based on theory of elasticity, bending curvature  $\phi$  is related to the moment diagram  $M$  by

$$\phi = \frac{M}{EI} \quad (6)$$

where  $EI$  is the flexural rigidity of the beam. Bending curvature is the second-order differential of the deflection  $\delta$ . Therefore the tangent of the deflection curve is

$$\frac{d\delta}{dx} = \int \phi dx + C \quad (7)$$

where  $C$  is a constant to be determined from the boundary condition. The deflection at any distance  $x$  from the left support may be calculated as

$$\delta(x) = \int_0^x \frac{d\delta}{dx} dx \quad (8)$$

At time  $t$ , the temperatures for the upper flange, web and lower flange of the section are known as  $T_1$ ,  $T_2$  and  $T_3$ . At the same time, the cross-section of the beam should satisfy two equilibrium conditions:

$$\sum_i N_i = 0 \quad (9)$$

$$\sum_i M_i = M(x) \quad (10)$$

where,  $N_i$  is the resultant axial force of the  $i^{\text{th}}$  component of the cross-section,  $M_i$  is the resultant bending moment of the  $i^{\text{th}}$  component of the cross-section to the neutral axis of the section and  $M(x)$  is the bending moment of the section due to the external load. From Eqs. (9) and (10), the neutral axis and the curvature of the section can be solved. If the curvature distribution along the whole beam length is known, the deflection can be calculated from Eqs. (7) and (8).

From Eq. (6), the curvature is proportional to the bending moment at normal temperature. It is reasonable to assume that the curvature is also proportional to the bending moment at elevated temperature. Eqs. (9) and (10) cannot be solved directly to obtain the neutral axis and curvature values. An iterative method must be used. In the following sections, the material model is firstly introduced and the iteration scheme is then explained.

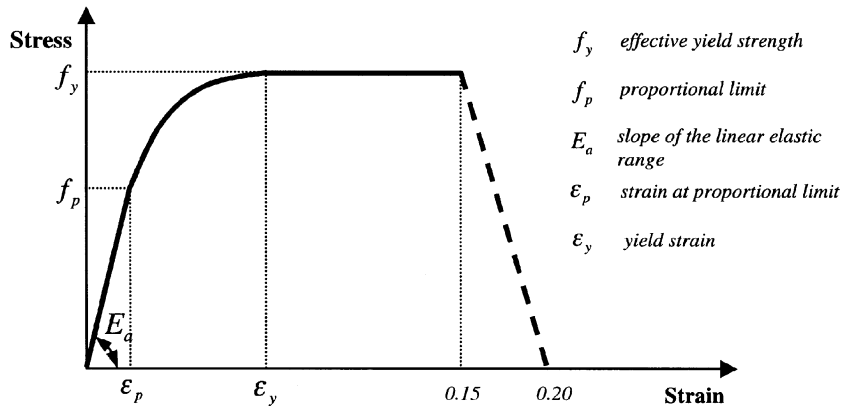
### 3.1. Material model

The mathematical model recommended by Eurocode 3: Part 1.2 (CEN 2001) offers a convenient way to express the stress-strain relationship of steel at elevated temperature. The original model consists of four ranges as shown in Fig. 5.

However, the expression for the transition range  $\varepsilon_p < \varepsilon < \varepsilon_y$  cannot be directly integrated. Its fourth order Taylor series at  $\varepsilon = 0.02$  is used instead. The proposed mathematical model for the transition range is

$$\sigma = f_p - c + b \left[ 1 - \frac{1}{2} \left( \frac{\varepsilon_y - \varepsilon}{a} \right)^2 - \frac{1}{8} \left( \frac{\varepsilon_y - \varepsilon}{a} \right)^4 \right] \quad (11)$$

Fig. 6 shows that the new mathematical model in general gives a good approximation to the EC3 stress-strain relationship although the stress at the beginning of the transition range is slightly over-predicted. However, its influence on the calculated deflection, as later shown in Section 3.5, is negligible.



Strain range	Stress	Parameters
$\epsilon \leq \epsilon_p$	$\sigma = \epsilon E_a$	$\epsilon_p = f_p / E_a$ $\epsilon_y = 0.02$ $a^2 = (\epsilon_y - \epsilon_p)(\epsilon_y - \epsilon_p + c/E_a)$ $b^2 = c(\epsilon_y - \epsilon_p)E_a + c^2$ $c = \frac{(f_y - f_p)^2}{(\epsilon_y - \epsilon_p)E_a - 2(f_y - f_p)}$
$\epsilon_p < \epsilon < \epsilon_y$	$\sigma = f_p - c + \frac{b}{a} \sqrt{a^2 - (\epsilon_y - \epsilon)^2}$	
$0.15 \geq \epsilon \geq \epsilon_y$	$\sigma = f_y$	
$0.2 > \epsilon > 0.15$	$\sigma = f_y \frac{0.2 - \epsilon}{0.05}$	

Fig. 5 The material model according to Eurocode 3: Part 2.1 (CEN 2001)

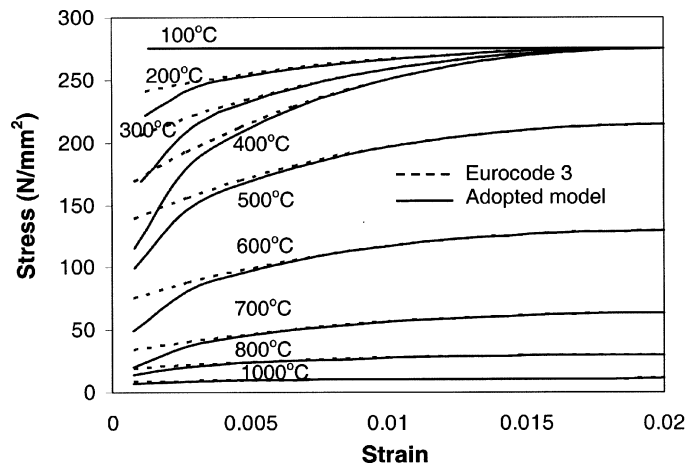


Fig. 6 Comparison of the Eurocode 3 and proposed model for the stress-strain relationship in the transition range,  $\epsilon_p < \epsilon < \epsilon_y$

### 3.2. Cross-section stress resultants

Once the neutral axis and section curvature are known, the resultant section force and moment can be calculated in the following way:

The I-section is divided into three rectangular plate components. For each plate component, the resultant axial force and moment can be obtained by integrating the stress and moment of the stress respectively as:

$$R_F(i) = p_w \times \int_{p_2}^{p_1} \sigma(T_i, p) dp \quad (12)$$

and

$$R_M(i) = p_w \times \int_{p_2}^{p_1} \sigma(T_i, p) p dp \quad (13)$$

where  $p_w$  is the width of that section component and  $p_1, p_2$  are distances of the two edges to the neutral axis (Fig. 7). Typical values of  $p_1, p_2$  and  $p_w$  of an I-section are listed in Table 1 and the neutral axis is defined as the distance to the upper edge of the section.

In view of Fig. 7, Eqs. (12) and (13) can be further written as

$$R_F(i) = p_w \times \left[ \int_0^{|p_1|} \sigma(T_i, p) dp - \int_0^{|p_2|} \sigma(T_i, p) dp \right] \quad (14)$$

and

$$R_M(i) = \begin{cases} p_w \times \left[ \int_0^{|p_1|} \sigma(T_i, p) p dp - \int_0^{|p_2|} \sigma(T_i, p) p dp \right] & p_1 > p_2 > 0 \\ p_w \times \left[ \int_0^{|p_1|} \sigma(T_i, p) p dp + \int_0^{|p_2|} \sigma(T_i, p) p dp \right] & p_1 > 0 > p_2 \\ p_w \times \left[ \int_0^{|p_2|} \sigma(T_i, p) p dp - \int_0^{|p_1|} \sigma(T_i, p) p dp \right] & 0 > p_1 > p_2 \end{cases} \quad (15)$$

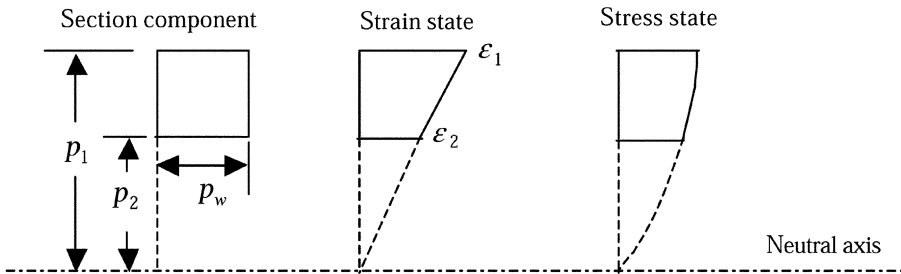


Fig. 7 Calculation of the resultant force and moment for a component plate in a cross section

Table 1 Parameters of the section components for I-section

Section component	Distance to neutral axis	Section plate width $p_w$
Upper flange	$p_1 = Z; p_2 = Z - t_f$	$w$
Web	$p_1 = Z - t_f; p_2 = Z - h + t_f$	$t_w$
Lower flange	$p_1 = Z - h + t_f; p_2 = Z - h$	$w$

Introducing the following functions:

$$F(T, p) = p_w \int_0^p \sigma(T, p) dp \quad p \geq 0 \quad (16)$$

$$M(T, p) = p_w \int_0^p \sigma(T, p) p dp \quad p \geq 0 \quad (17)$$

Eqs. (14) and (15) become

$$R_F(i) = F(T_i, |p_1|) - F(T_i, |p_2|) \quad (18)$$

$$R_M(i) = \begin{cases} M(T_i, |p_1|) - M(T_i, |p_2|) & p_1 > p_2 > 0 \\ M(T_i, |p_1|) + M(T_i, |p_2|) & p_1 > 0 > p_2 \\ M(T_i, |p_2|) - M(T_i, |p_1|) & 0 > p_1 > p_2 \end{cases} \quad (19)$$

If linear strain distribution is assumed, (i.e. plane section remains plane after deformation), the strain of a section point is related to its distance from the neutral axis by

$$\varepsilon = \phi \times p \quad (20)$$

where  $\phi$  is the curvature and  $p$  is the distance of the section point to the neutral axis.

Substituting Eq. (20) into the material model of section 3.1 relates the stress of any section point to its distance from the neutral axis  $p$  and temperature  $T$ :

$$\sigma = \begin{cases} E_{a,T} p / \phi & < p \leq \varepsilon_p / \phi \\ f_{p,T} - c + b \left[ 1 - \frac{1}{2} \left( \frac{0.02 - p / \phi}{a} \right)^2 - \frac{1}{8} \left( \frac{0.02 - p / \phi}{a} \right)^4 \right] & \varepsilon_p / \phi < p < 0.02 / \phi \\ f_{y,T} & 0.02 / \phi \leq p \leq 0.15 / \phi \\ f_{y,T} \frac{0.2 - p / \phi}{0.05} & 0.15 / \phi < p < 0.2 / \phi \end{cases} \quad (21)$$

Substituting Eq. (21) into Eqs. (16) and (17) gives the expressions for  $F(T, p)$  and  $M(T, p)$ , the details of which are given in the appendix.

The total resultant force and moment for the section is the sum of the resultant force and moment for each plate component. For I- and H-section beams, the following expressions apply:

$$R_F = \sum_{i=1}^3 R_F(i) \quad (22)$$

$$R_M = \sum_{i=1}^3 R_M(i) \quad (23)$$

### 3.3. Iteration scheme for solving the section curvature

The basic principle involved in the iterative scheme is that the curvature from the previous time step is used as the trial value of the current time step. The neutral axis for the previous time step is then used to calculate the resultant force of the section. If the resultant axial force is not zero, the neutral axis is shifted until Eq. (9) is satisfied within a predefined tolerance. Finally the resultant moment for the converged neutral axis is calculated. According to the assumption that the curvature is proportional to the bending moment, the curvature for the maximum moment section should be

$$\phi_{\max} = \frac{M_{\max}}{R_M} \phi \quad (24)$$

where  $\phi$  is the current curvature. The curvature  $\phi_{\max}$  from Eq. (24) may not satisfy  $R_M = M_{\max}$  because the curvature may not be strictly proportional to the bending moment. However, it makes  $R_M$  closer to  $M_{\max}$ . A new iteration begins until both Eqs. (9) and (10) are satisfied within a predefined tolerance. The initial neutral axis of a symmetric cross-section is located at the half-depth  $h/2$ , while the initial maximum curvature can be calculated from structural elasticity as

$$\phi_{\max,0} = \frac{M_{\max}}{EI} \quad (25)$$

where  $M_{\max}$  is the maximum bending moment along the beam length and  $EI$  is the flexural rigidity at normal temperature.

### 3.4. Mechanical deflection

When the maximum curvature is solved, the beam deflection is calculated as

$$\delta_m = kL^2 \phi_{\max} \quad (26)$$

where  $k$  is a factor determined from the moment distribution. For example,  $k$  is 1/12 for beams having one point load at the mid-span point and 5/48 for beams carrying a uniformly distributed load.

### 3.5. Thermal deflection

As the lower flange of floor beams are heated to a higher temperature than the upper flange, an additional deflection will be induced by the non-uniform expansion of the section (Usmani *et al.* 2001). Assuming an uniform temperature gradient along the beam length as

$$dT = (T_3 - T_1)/h \quad (27)$$

The corresponding curvature induced along the length of the beam may be written as

$$\phi_T = \alpha \times dT \quad (28)$$

where  $\alpha$  is the thermal expansion coefficient. The total rotation angle for a beam of length  $L$  is

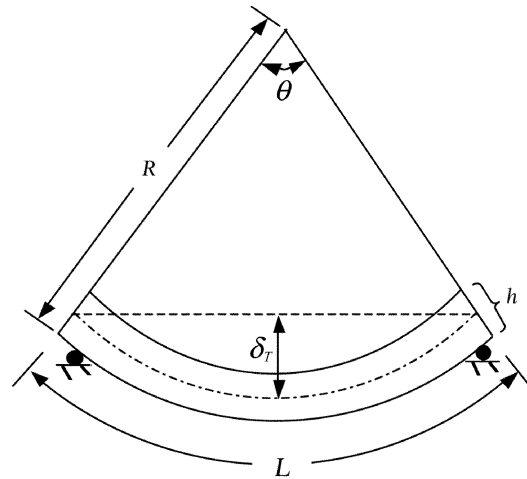


Fig. 8 Deflection due to thermal bowing effect

$$\theta = \phi_T \times L \quad (29)$$

and the mid-span deflection due to the temperature gradient is (Fig. 8)

$$\delta_T = [1 - \cos(\phi L/2)]/\phi \quad (30)$$

The total deflection of simply-supported beams is the sum of mechanical deflection (Eq. 26) and thermal deflection (Eq. 30).

$$\delta = \delta_m + \delta_T \quad (31)$$

### 3.6. Verification studies

A total of fourteen tests involving five beam sizes were done on simply-supported steel beams supporting a concrete slab in the British standard tests (Wainman and Kirby 1987). The steel beams were non-composite, i.e., there was no shear connector between the beam and the slab. The beam deflections calculated using the proposed method are compared with the test results. Selected temperature-deflection curves for three beam sizes are shown in Figs. 9(a)-(c). Comparisons of tests and predicted results show a similar trend that the calculated deflection is slightly higher than the test results at the initial range and then become slightly lower. Nevertheless, the maximum difference in deflection does not exceed 10 mm. At collapse, the calculated deflections increase rapidly and the predicted limiting temperatures are 50-100 °C lower than the test results. This is expected because the nominal design strength is used in the theoretical calculation while the real material strength should be somewhat higher than the assumed design strength. The other reason that explains the earlier failure of the predicted results is that the web temperature is assumed to be uniform and equal to the maximum value. In reality, the temperature at the upper end of the web will be lower, whose influence, although negligible, could be significant when the beam approaches failure. The same analysis is also performed

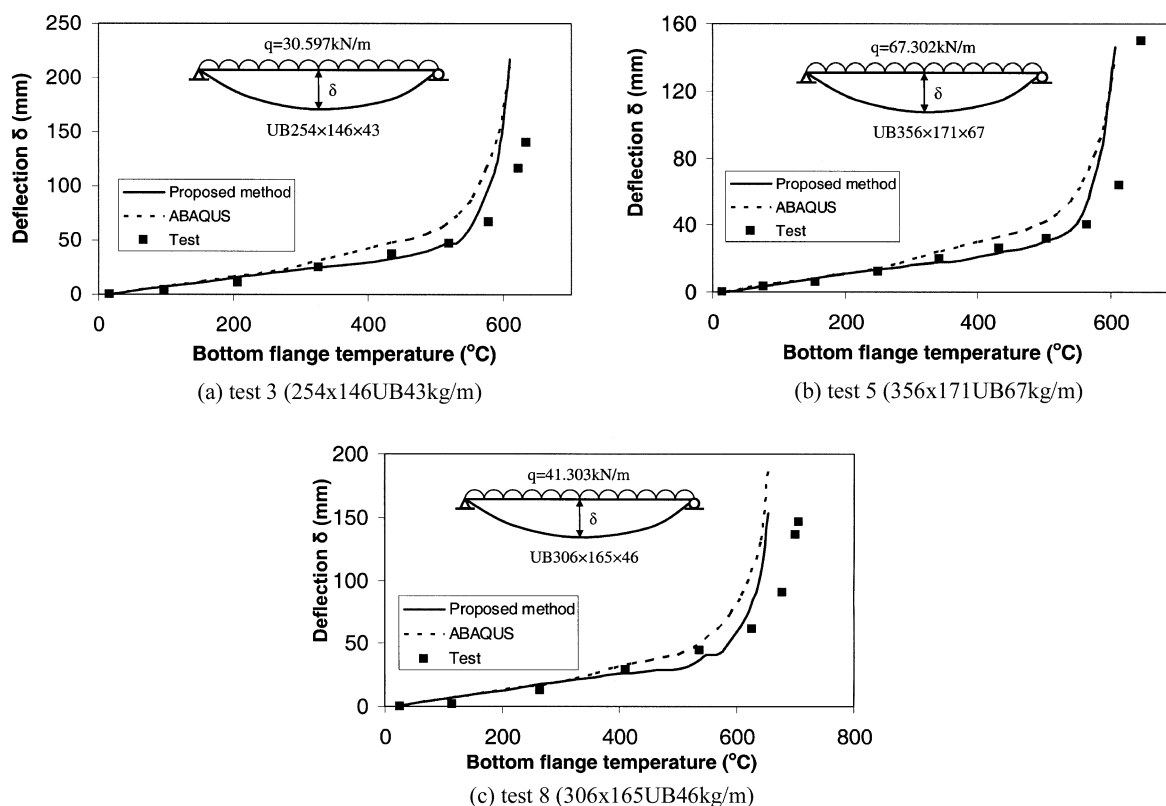


Fig. 9 Comparison of the calculated results and test results with ABAQUS results (Wainman and Kirby 1987, test 1)

by nonlinear finite element analysis program ABAQUS, in which the nominal design strength is used and uniform temperature is assumed for section plate component. Comparison of results show that the proposed method gives the same initial deflection and ultimate failure temperature as predicted by ABAQUS. In the intermediate heating range, beam deflection from the proposed method is smaller than ABAQUS results which may be due to the over-calculation of the stress in the transition range. However, the predicted values are closer to the test results.

#### 4. Fire safety design of steel beams

There are two main considerations for the design of floor beams in fire. One is the strength requirement in which the load carrying capacity of the member cannot be exceeded. The other is deformation requirement, or the displacement of the beam must be limited to avoid damage to structural or non-structural components. To satisfy the second requirement, a deflection limit is normally specified and the temperature at which the predefined deflection limit is reached is deemed as the limiting temperature. However, from experimental observation, there is no clear indication of beam losing its load bearing capacity when exposed to fire. The tests were often terminated when the deformation exceeds certain criterion to avoid damage to the test furnace.

The beam stiffness is the key parameter that affects the beam deflection. It can be observed from Fig. 5 that when the strain of the beam flange reaches its effective yield strain, the beam loses its stiffness rapidly and collapse is almost immediate. The proposed moment-curvature method is adopted to study the response of steel beams exposed to fire. In the proposed method, the neutral axis  $Z$  and the curvature  $\phi$  of the section at the maximum moment location can be calculated and the maximum strain at the bottom of the beam flange can be obtained as (Fig. 2),

$$\varepsilon_{\max} = (h - Z)\phi \quad (32)$$

It is proposed that the limiting temperature be defined as the temperature when the maximum strain  $\varepsilon_{\max}$  in the cross section reaches the effective yield strain of 2% in accordance with EC3: Part 1.2.

BS476 (BSI 1987) also recommends a performance criterion for the load-bearing capacity of bending members when exposed to standard fire. Flexural members are deemed to have lost its load-bearing capacity when the following criteria are violated (BSI 1987):

- a. Deflection,  $\delta < L / 20$ , or
- b. Rate of deflection,  $R < L^2 / (9000 \text{ h})$  in mm/min

where  $L$  is the clear span and  $h$  is the beam depth. The rate of deflection limit should not apply before a deflection of  $L/30$  is exceeded.

Most of the tests carried out on steel beams exposed to fire do not allow the beams to deflect to a very extent and hence the ultimate failure temperature at which the collapse of beam occurred cannot be recorded. Therefore it is not possible to deduce from the test records what is the “actual” failure temperature of the beam. However, numerical analysis can be continued until the deflection becomes numerically infinity. The nonlinear finite element analysis program, ABAQUS, is used to check the accuracy of the proposed method in determining the critical temperature. The critical temperature predicted by ABAQUS is taken as when the maximum beam deflection becomes  $L/5$  which is deemed as sufficiently large for the ultimate failure of beams to occur. In the following sub-sections, the critical temperature obtained based on effective yield strain of 2% is compared to the BS476 criteria and they are checked with the results predicted by ABAQUS for beams with different span lengths, load ratios, beam sizes and loadings.

#### 4.1. Effect of load ratios

The parametric study is conducted on a simply-supported beam of 254×146UB43 Grade 275 steel, length 4.5 m and 6 m and subjected to a uniformly distributed load. The loads are varied with load ratio ranging from 0.3 to 0.8. The results, presented in Table 2, show that the proposed failure criterion based on effective yield strain of 2% gives the limiting temperature closer to the ultimate failure temperature predicted by ABAQUS. Although the proposed method gives conservative prediction when compared to the ABAQUS results, the maximum temperature difference is within 13°C for a wide range of load ratios. In contrast, the limiting temperature given by BS476 is more conservative when the load ratio is increased and a maximum difference of 70°C was observed for beam length 6m and load ratio 0.8.

Table 2 Prediction of failure temperature for beam UB254×146×43 kg/m with various load ratios and span lengths

Span length	Load ratio	Limiting temperature (°C)				
		ABAQUS failure temperature (1)	BS476 Criteria (2)	Difference (1)-(2)	2% yield strain criterion (3)	Difference (1)-(3)
4.5 m	0.3	695	685	10	690	5
	0.4	659	648	11	654	5
	0.5	620	605	15	613	7
	0.6	588	568	20	580	8
	0.7	560	529	31	547	13
	0.8	524	480	44	513	11
6.0 m	0.3	695	676	19	691	4
	0.4	660	635	25	654	6
	0.5	620	593	27	613	7
	0.6	587	555	32	580	7
	0.7	559	514	45	547	12
	0.8	523	453	70	513	10

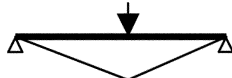
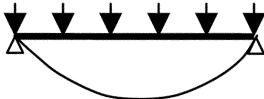
4.2. Effects of beam size and span length

In this study, the beam size and span length are varied and the limiting temperatures predicted by the three methods are compared. The results are shown in Table 3. In the first series of the study, the beam span is kept at 6.0 m while the beam size varies. In the second series, beam size UB356×171×67 is fixed while the span length varies from 4.0 m to 8.0 m. The load ratio for all the beams is kept at 0.5. According to the BS476 method, change of the beam geometry should have no effect on the limiting temperature. However, the analysis results from ABAQUS show that the limiting temperature increases when the section size is larger. The span length should not have any effects as long as the load ratio

Table 3 Comparison of the failure temperature for beams with different beam sizes and span lengths (load ratio = 0.5)

Beam attributes		Limiting temperature (°C)				
		ABAQUS failure temperature (1)	BS476 criteria (2)	Difference (1)-(2)	2% yield strain criterion (3)	Difference (1)-(3)
Beam size (L = 6 m)	UB254×146×43	618	591	27	612	6
	UB305×165×54	619	600	19	613	6
	UB356×171×67	623	609	14	616	7
	UB406×178×74	627	615	12	620	7
	UB457×191×98	628	619	9	620	8
Beam span, L (UB356×171×67)	4.0 m	622	616	6	615	7
	5.0 m	622	613	9	615	7
	6.0 m	622	607	15	615	7
	7.0 m	622	600	22	615	7
	8.0 m	622	595	27	615	7

Table 4 Comparison of the three criteria with respect to the loading type

Loading type	Failure temperature based on plastic analysis (°C) (1)	BS476 (°C) (2)	Difference (°C) (1)-(2)	2% Ultimate strain criterion (°C) (3)	Difference (°C) (1)-(3)
	622	613	9	615	7
	622	607	15	615	7
	622	598	24	615	7

remains the same. The deflection criteria given by BS476 seem to predict different limiting temperature for beams with the same load ratio but different span length. On the other hand, the limiting temperature predicted by the 2% effective yield strain criterion gives a consistency and better prediction of beams failure temperature compared to the nonlinear finite element analysis showing a small difference of 6 to 8°C.

#### 4.3. Other loading conditions

In the plastic theory, the limiting temperature is defined as the temperature at which, the plastic resistance of the section equals to the maximum bending moment of the beam. Therefore, it is independent of the bending diagram. In this section, three typical moment diagrams generated by various loading conditions are studied. The load magnitudes are controlled so that the moment diagrams are different but the maximum moments are the same. The load ratio is around 0.5. The nonlinear finite element results given by ABAQUS show that although the temperature-deflection curves for these three beams are different, they fail at the same temperature as shown in Table 4. This is in agreement with the plastic theory. In the moment-curvature method proposed in this paper, the maximum strain is calculated according to the maximum moment. The effect of moment diagram is only considered when calculating the mid-span deflection. Therefore, it is able to give uniform limiting temperatures for all three loading types. However, the limiting temperature given by BS476 is loading type dependent.

#### 4.4. Fire safety design of beams

The studies show that the proposed ultimate strain criterion can accurately predict the failure temperature with a consistent error of around 7°C for beams with various span lengths, section sizes and loading conditions. Therefore, the 2% effective yield strain criterion is proposed for use in situations where only the ultimate strength limit state governs the design. For beams that are sensitive to deflection, the moment-curvature method may be used to predict the total deflection including the effect of thermal bowing. The recommended procedure for fire safety design of floor beam is shown in the flow chart in Fig. 10.

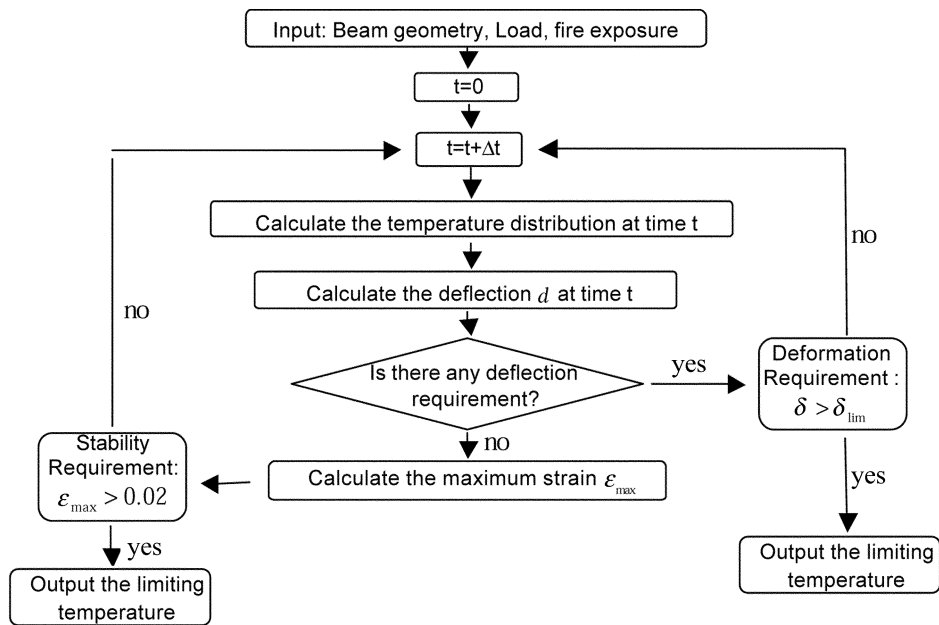


Fig. 10 An integrated approach for fire safety design of steel beams

## 5. Conclusions

This paper proposes some improvements to the EC4 method for estimating the temperature distribution in a beam that supports a concrete slab, and the improved method provides a better estimation of the beam deflection when compared to the established test results. Based on the calculated temperature, an iteration scheme is used to determine the neutral axis and the curvature of the beam section satisfying the force equilibrium in the cross section. The total beam deflection, including both the mechanical and thermal bowing deflections, can be evaluated.

The beam deflection calculated from the proposed method is verified against the British standard tests for 3-side heated floor beams. The results show that the proposed method gives very close estimation of the test results except that the ultimate temperature is under estimated by 30-50°C. The results are also compared with those obtained from nonlinear finite element analysis and good agreement is observed. The proposed method may be used to evaluate the beam response for general loading and fire exposure conditions.

In cases where beam deflection is not the main concern for fire safety design, it is proposed that the limiting temperature should be determined from the maximum strain in the cross section reaching a value of 2%. Extensive studies on floor beams with various load ratios, beam sizes, span lengths and load types show that the failure criterion based on 2% effective yield strain can be used to predict the limiting temperature with better accuracy when compared to the current deflection criteria recommended by BS476. For all the cases studied, the limiting temperature predicted by the proposed yield strain criterion is within 7°C from the ultimate failure temperature obtained from the nonlinear finite element analysis. Finally, an integrated design procedure considering both ultimate strength and deflection limit states is proposed for fire safety design of floor beams.

## References

- Buchanan, A.H. (2001), *Structural Design for Fire Safety*, Chichester, John Wiley & Sons, 108-113.
- BSI (1987), BS476, *Fire Tests on Building Materials and Structures, Part 20: Methods for Determination of the Fire Resistance of Elements of Construction (General Principles)*, British Standards Institution, London, UK.
- BSI (2000), BS5950, *Structural Use of Steelwork in Building: Part 8. Code of Practice for Fire Resistant Design*, British Standards Institution, London, UK.
- European Committee for Standardization (CEN) (1996), *DD ENV 1991-2-2, Eurocode 1: Basis of design and actions on structures. Part 2.2, Actions on structures exposed to fire*, British Standards Institution, UK.
- European Committee for Standardization (CEN) (2001), *DD ENV 1993-1-2, Eurocode 3: Design of steel structures. Part 1.2, General rules - Structural fire design*, British Standards Institution, UK.
- European Committee for Standardization (CEN) (2002), *Draft PrEN 1994-1-2, Eurocode 4: Design of Composite Steel and Concrete Structures, Part 1.2: Structural Rules- Structural Fire Design*, British Standard Institution.
- Franssen, J.M. Cooke, G.M.E. and Latham, D.J. (1995), "Numerical simulation of a full scale fire test on a loaded steel framework", *J. Const. Steel Res.*, **35**, 377-408.
- Huang, Z., Burgess, I.W. and Plank, R.J. (2004), "Fire resistance of composite floors subject to compartment fires", *J. Const. Steel Res.*, **60**, 339-360.
- Lawson, R.M. and Newman G.M. (1996), *Structural Fire Design to EC3 & EC4, and comparison with BS 5950*, Technical Report, SCI Publication 159, the Steel Construction Institute.
- Li, G.Q, He, L.J. and Jiang, S.C. (2000), "Fire resistance experiments and theoretical calculation of a restrained steel beam", *China Civil Engineering Journal*, **33**, 23-26.
- Li, G.Q. and Jiang, S.C. (1999), "Prediction to nonlinear behavior of steel frames subjected to fire", *Fire Safety Journal*, **32**, 347-368.
- Liew, J.Y.R., Tang, L.K., Holmaas, T. and Choo, Y.S. (1998), "Advanced analysis for the assessment of steel frames in fire", *J. Const. Steel Res.*, Elsevier Science, UK, **47**(1-2), 19-45.
- Liew, J.Y.R., Tang, L.K. and Choo, Y.S. (2002), "Advanced analysis for performance-based design of steel structures exposed to fires", *J of Struct. Eng.*, ASCE, **128**(12), 1584-1593.
- Liu, T.C.H., Fahad, M.K. and Davies, J.M. (2002), "Experimental investigation of behaviour of axially restrained steel beams in fire", *J. Const. Steel Res.*, **58**, 1211-1230.
- Liew, J.Y.R. (2004), "Performance based fire safety design of structures - A multi-dimensional integration", *Advances in Structural Engineering*, Multi-Science Publisher, U.K, **7**(4), 111-133.
- Ma, K.Y. and Liew, J.Y.R. (2004), "Nonlinear plastic hinge analysis of 3-D steel frames in fire", *J. Struct. Eng.*, ASCE, July, In Press.
- Twilt, L. (2001), "The new Eurocode on fire design of steel structures", In *Proc. of the Int. Seminar on Steel Structures in Fire*, November 2001, Shanghai China, 241-254.
- Usmani, A.S., Rotter, J.M., Lamont, S.S. and Gillie, M. (2001), "Fundamental principles of structural behaviour under thermal effects", *Fire Safety Journal*, **36**, 721-744.
- Wainman, D.E. and Kirby, B.R. (1987), "Compendium of UK standard fire test data unprotected structural steel", British Steel Corporation and Swinden Laboratories, Rotherham, Report RS/RSC/s10328/1/87/B.
- Wang, Y.C. (2001), "A review of the behaviour of steel structures in fire and a suggestion for future experimental research studies", In *Proc. of International Seminar on Steel Structures in Fire*, November 2001, Shanghai, China.
- Wang, Y.C. (2002), *Steel and Composite Structures Behaviour and Design for Fire Safety*, London and New York, Spons Press, 175-179.
- Wong, M.B. (2001), "Comparison of heat transfer procedures for frame design under fire conditions", In *Proc. of International Seminar on Steel Structures in Fire*, November, 2001, Shanghai, China.
- Wong, M.B., Ghojel, J.I. (2003), "Sensitivity analysis of heat transfer formulations for insulated structural steel components", *Fire Safety Journal*, **38**, 187-201.

## Appendix

The expression for the stress as a function of distance to the neutral axis  $p$  as shown in Eq. (21) constitutes of four ranges. Therefore, function  $F(T, p)$  and  $M(T, p)$  as an integration of the stress over the section could be consisted of four parts depending on the value of  $p$ .

The expression for  $F(T, p)$  is

$$F(T, p) = \begin{cases} p_w L(T, p) & p \leq \varepsilon_p / \phi \\ p_w [L(T, \varepsilon_p / \phi) + Tr(T, p)] & \varepsilon_p / \phi < p < 0.02 / \phi \\ p_w [L(T, \varepsilon_p / \phi) + Tr(T, 0.02 / \phi) + P(T, p)] & 0.02 / \phi \leq p \leq 0.15 / \phi \\ p_w [L(T, \varepsilon_p / \phi) + Tr(T, 0.02 / \phi) + P(T, 0.15 / \phi) + D(T, p)] & 0.15 / \phi < p < 0.2 / \phi \end{cases}$$

where

$$L(T, x) = E_a(T) \phi x^2 / 2$$

$$Tr(T, x) = \frac{a}{120 \phi} [120(c - f_p(T))(\Delta_x - \Delta_1) - b(120(\Delta_x - \Delta_1) - 20(\Delta_x^3 - \Delta_1^3) - 3(\Delta_x^5 - \Delta_1^5))] ]$$

where  $\Delta_x = \frac{(0.02 - x/\phi)}{a}$ ;  $\Delta_1 = \frac{(0.02 - \varepsilon_p(T))}{a}$

$$P(T, x) = f_y(T) \left( x - \frac{0.02}{\phi} \right)$$

$$D(T, x) = f_y(T) \left( 4 \left( x - \frac{0.15}{\phi} \right) + 10 \left( \left( \frac{0.15}{\phi} \right)^2 - x^2 \right) \right)$$

The expression for  $M(T, P)$  is

$$M(T, p) =$$

$$\begin{cases} p_w ML(T, p) & p \leq \varepsilon_p / \phi \\ p_w [ML(T, \varepsilon_p / \phi) + MTr(T, p)] & \varepsilon_p / \phi < p < 0.02 / \phi \\ p_w [ML(T, \varepsilon_p / \phi) + MTr(T, 0.02 / \phi) + MP(T, p)] & 0.02 / \phi \leq p \leq 0.15 / \phi \\ p_w [ML(T, \varepsilon_p / \phi) + MTr(T, 0.02 / \phi) + MP(T, 0.15 / \phi) + MD(T, p)] & 0.15 / \phi < p < 0.2 / \phi \end{cases}$$

where

$$ML(T, x) = E_a(T) \phi x^3 / 3$$

$$MTr(T, x) = \frac{a}{240\phi^2} \left[ b \left( \begin{array}{l} 120(c - f_p(T))(\Delta_x - \Delta_1)(\varepsilon_y^2(T) - a(\Delta_x + \Delta_1)) + \\ \varepsilon_y(T)(240(\Delta_1 - \Delta_x) - 40(\Delta_1^3 - \Delta_x^3) - 6(\Delta_1^5 - \Delta_x^5)) + \\ 5a(-24(\Delta_1^2 - \Delta_x^2) + 6(\Delta_1^4 - \Delta_x^4) + (\Delta_1^6 - \Delta_x^6)) \end{array} \right) \right]$$

$$MP(T, x) = \frac{f_y(T)}{2} \left( x^2 - \left( \frac{0.02}{\phi} \right)^2 \right)$$

$$MD(T, x) = 20 f_y(T) \left( \frac{0.15}{2} \left( x^2 - \left( \frac{0.15}{\phi} \right)^2 \right) - \frac{\phi}{3} \left( x^3 - \left( \frac{0.15}{\phi} \right)^3 \right) \right)$$

SC